Global properties and propensity to dimerization of the amyloid-beta (12-28) peptide fragment through the modeling of its monomer and dimer diffusion coefficients and electrophoretic mobilities.

Julio A. Deiber[1], Marta B. Peirotti[1], Maria V. Piaggio[2]

[1]Instituto de Desarrollo Tecnológico para la Industria Química (INTEC), Universidad Nacional del Litoral (UNL), Consejo Nacional de Investigaciones Científicas y Técnicas (CONICET), Santa Fe, Argentina

[2]Cátedra de Bioquímica Básica de Macromoléculas, Facultad de Bioquímica y Ciencias Biológicas, UNL, Santa Fe, Argentina

Running title: Properties and propensity to dimerization of amyloid-beta (12-28)

Correspondence: Dr. Julio A. Deiber, INTEC, Güemes 3450, 3000, Santa Fe, Argentina

E-mail: treoflu@santafe-conicet.gov.ar

Fax: +54-(0)342-4550944

Received: 12-Aug-2014; Revised: 20-Oct-2014; Accepted: 05-Nov-2014

This article has been accepted for publication and undergone full peer review but has not been through the copyediting, typesetting, pagination and proofreading process, which may lead to differences between this version and the Version of Record. Please cite this article as doi: 10.1002/elps.201400395.

Abbreviations: AAS, amino acid sequence; **Aβ**, amyloid-beta; **AD**, Alzheimer´s Disease; **IPCR**, intraparticle charge regulation; **PLLCEM**, Perturbed Linderstrøm-Lang Capillary Electrophoresis Model; **PPCR**, pair particle charge regulation.

Key words: amyloid-beta fragment / charge regulation phenomena / dimerization equilibrium / effective electrophoretic mobility / translational diffusion coefficient

Manuscript total number of words and figure legends is 5531

Abstract

Neuronal activity loss may be due to toxicity caused mainly by amyloid-beta (1-40) and (1-42) peptides forming soluble oligomers. Here the amyloid-beta (12-28) peptide fragment (monomer) and its dimer are characterized at low pH through the modeling of their diffusion coefficients and effective electrophoretic mobilities. Translational diffusion coefficient experimental values of monomer and dimer analogues of this peptide fragment and monomer and dimer mixtures at thermodynamic equilibrium are used as reported in the literature for different monomer initial concentrations. The resulting electrokinetic and hydrodynamic global properties are employed to evaluate the amyloid-beta (12-28) peptide

fragment propensity to dimerization through a thermodynamic theoretical framework. Therefore equilibrium constants are considered at pH 2.9 to elucidate one of the amyloidogenic mechanisms involving the central hydrophobic region LVFFA of the peptide spanning residues 17-21 associated with phenylalanine at positions 19 and 20 in the amino acid sequence of amyloid-beta peptides. An analysis demonstrating that peptide aggregation is a concentration-dependent process is provided, where both pair and intraparticle charge regulation phenomena become relevant. It is shown that the modeling of the effective electrophoretic mobility of the amyloid-beta (12-28) peptide fragment is crucial to understand the effect of hydrophobic region LVFFA in the amyloidogenic process.

1 Introduction

Global electrokinetic and hydrodynamic properties of peptides are needed to find out key biophysical mechanisms associated with bioprocesses involved in human pathologies (see for instance Refs. [1-4]). In this regard, the amyloidogenic process found in Alzheimer´s Disease (AD) is a relevant case study [4]. At present the definite etiopathology of AD is not well known [5, 6], although several hypotheses have been proposed, and among them, the loss of neuronal activity due to toxicity caused by amyloid-beta (Aβ) peptides forming soluble aggregates is considered one of the most probable. In fact the histopathology is characterized by extracellular plaques formation caused by aggregation of mainly Aβ(1-42) with an amino acid sequence (AAS) DAEFRHDSGYEVHHQKLVFFAEDVGSNKGAIIGLMVGGVVIA, and Aβ(1-40) where the terminal I(41) and A(42) are not present [4, 5]. In previous studies emphasis has been placed on the fact that an increase in Aβ soluble oligomers, intermediates, and fibrils with a progressive formation of amyloid plaques was found, where addition of new aggregates occurred. Nevertheless the specific molecular mechanisms yielding extracellular plaques are not well understood yet. In a previous work we have shown [4] that electrokinetic and hydrodynamic properties of Aβ peptides evaluated from the modeling of their effective electrophoretic mobilities at well defined BGE properties were required to estimate the propensity to aggregation of these polyampholyte-

polypeptide chains having weak ionizing groups. It was shown that CE is one of the most appropriate experimental methods to achieve the evaluation of a well defined set of global properties needed in calculations involving peptide Brownian aggregation theories [4]. Also it was pointed out that Aβ peptide concentration, aggregate sizes and near molecule pH due to the pair particle charge regulation (PPCR) phenomenon might be crucial parameters in the amyloidogenic process. The PPCR phenomenon is a relevant and still no well described effect in polypeptide interactions, which must be added to the classical intraparticle charge regulation (IPCR) phenomenon [7-12] giving the near molecule pH designated pH^* [4]. In the present work we continue this study concomitantly with another relevant experimental work [13] on this subject. Now the focus is placed on the propensity to dimerization of the amyloid-beta (12-28) peptide fragment. The rationale is that phenylalanine at positions 19 and 20 in the AAS of Aβ peptides may be a zone of nucleation in the oligomerization process. Since some peptides contain specialized domains enhancing dimerization, we will refer to the homo-dimerization of the Aβ(12-28) peptide fragment common to most Aβ peptide AASs relevant in AD. Further an analysis concerning the effect of initial monomer concentration on this peptide aggregation will be provided.

It is worth to observe that basic transport properties like diffusion and friction coefficients, intrinsic viscosity and electrophoretic mobility are interconnected

through some common phenomenological aspects, among which chain friction is the relevant information sensitive to hydration, size and shape of peptides visualized as different types of hydrodynamic particles [14, 15]. In particular the electrophoretic mobility is proportional to the effective charge number of ionizing groups in the AAS presenting a challenging for screening out the electrokinetic and hydrodynamic phenomena involved in the polyampholyte-polypeptide heterochains [3, 4, 7-12, 14-29]. The comprehension of the interplay among these transport properties through rigorous models is useful in modern biotechnology as described previously in many publications. Their measurements through different analytical techniques like for instance CE [30-34] at well defined temperature T, pH, ionic strength I, electrical permittivity ε and viscosity η_s, are valuable results for studying biophysical mechanisms and process.

This work presents the evaluation of global properties of monomer and dimer analogues of the Aβ(12-28) peptide fragment. For this purpose, experimental data of translational diffusion coefficient for monomer and dimer analogues and monomer and dimer mixtures at thermodynamic equilibrium provided by Ref. [13] were modeled to estimate the friction coefficients of these hydrated particles. In fact, monomer and dimer analogues were obtained so that diffusion coefficient measurements could be carried out avoiding monomer dimerization and conversely impeding dimer reversion to monomer. Further, diffusion

coefficients of the monomer and dimer mixtures were obtained from the Aβ(12-28) peptide fragment at different initial monomer concentrations. This interesting proposal provided valuable experimental information to visualize the propensity to dimerization of the Aβ(12-28) peptide fragment in the present work. In fact, friction coefficients were calculated via our previous theoretical developments [12, 14], which then allowed us the estimation of the corresponding effective electrophoretic mobilities. Although it is preferable to use directly effective electrophoretic mobilities values obtained from CE [30-34], this method has not been exploited appropriately for this type of subject despite it is offering the relevant experimental information as already indicated in the literature [4, 35-42]. Here we find this alternative valid because the Perturbed Linderstrøm-Lang Capillary Electrophoresis Model (PLLCEM) [7-12, 14, 15, 22, 25-27] may be also applied when the input data is the diffusion coefficient value (Supporting Information). This model provides electrokinetic and hydrodynamic properties necessary to study the equilibrium between monomer and dimer and to evaluate the associated total free energy change. For this purpose, the thermodynamic theory established previously [9, 43] was used as modified and presented below for the case of monomer and dimer thermodynamic equilibrium.

In this work, Section 2 is split in two parts: (i) Section 2.1 describes the monomer, dimer and their analogues, and the experimental information used here. (ii) Section 2.2 presents theoretical thermodynamic considerations of peptide dimerization involving electrokinetic and hydrodynamic global properties obtained from the PLLCEM for different initial monomer concentration. Section 3 discusses results of the dimerization process placing emphasis on the effect of the IPCR and PPCR phenomena. Finally Section 4 provides concluding remarks and suggestions for future researches.

2 Materials and methods

2.1 The Aβ(12-28) peptide fragment and diffusion coefficient experimental data

For the purpose of using a non-aggregating monomer analogue at low pH in Ref. [13], the monomer AAS expressed VHHQKLVFFAEDVGSNK was changed to VHHQKLVGGAEDVGSNK designated here monomer analogue and coded as [$G^{19,20}$]Aβ(12-28). Thus the FF at position 19 and 20 of the Aβ(1-42) peptide were changed to GG. Also to use a non-reverting dimer analogue, a modified dimer was generated through a disulfide-linked bond of two monomer analogues. These mutated monomer analogues had each one the F at position 20 changed to C giving the dimer analogue $(VHHQKLVFCAEDVGSNK)_2$ coded as $([C^{20}]Aβ(12-28))_2$ in [13]. The diffusion coefficient of the mixture was composed of monomer and dimer indicating that the interconversion between

these species at equilibrium was a rapid kinetic process thus providing one mixture diffusion coefficient value only (see also discussion in [13] and below). Thus peptide chains are sampling rapidly both states giving weighed average values of mixture diffusion coefficients. Therefore experimental diffusion coefficients of these peptides solutions were obtained at 25ºC via pulsed-field gradient nuclear magnetic resonance spectroscopy. The peptides were dissolved in D_2O adjusted to pD 2.9 with DCl giving an ionic strength $I \approx 1$ mM. Peptide solutions were prepared in the range $C_o = 0.5\text{-}3.25$ mM by serial dilution. For $C_o > 3.25$ mM the peptide fragment solubility was highly diminished. Experimental values of monomer and dimer mixture diffusion coefficient D of Aβ(12-28) peptide fragment reported in Ref. [13] was fitted through the polynomial $D \approx (2.4432 - 0.1955C_o + 0.0224C_o^2) \times 10^{-10}$ m^2/s with a correlation coefficient $r^2 \approx 0.97$. Further, the monomer $D_M = 2.48 \times 10^{-10}$ m^2/s and dimer $D_D = 1.78 \times 10^{-10}$ m^2/s diffusion coefficient analogues were provided, which in principle were independent from C_o within the concentration range studied [13]. D_2O properties required in our calculations are available in the Supporting Information. The Aβ(12-28) peptide fragment, like Aβ(1-40) and Aβ(1-42) peptides, forms amyloid fibrils in vitro for pH>4. One reason is that their chain negative and positive ionizing groups may form salt bridges stabilizing the β-sheet formations. Nevertheless at pH 2.9, the Aβ(12-28) has a positive effective

charge number while the residual and terminal carboxylic groups are partially protonated producing dimers driven by hydrophobic forces [13].

2.2 Theoretical concepts and considerations

2.2.1 The Aβ(12-28) peptide fragment dimerization from the thermodynamic point of view

In general the oligomerization of peptide chains is a concentration-dependent process that may be visualized from different thermodynamics and kinetics theories [4, 13]. Here we will refer to the dimerization process of Aβ(12-28) peptide fragments at pH 2.9 where equilibrium between monomer and dimer structures can be found [13]. Therefore, monomer and dimer (species $\alpha = \mathrm{M}, \mathrm{D}$) follow the dimerization stoichiometry $2\,\mathrm{M} \leftrightarrow \mathrm{D}$. Defining X_α as the molar fraction of species α, the dimerization equilibrium constant is $K = X_D / X_M^2$. The chemical potentials G_α of these polyampholyte-polypeptide chains with N_α amino acid residues are required. G_α are associated with the conformations of chains in the BGE and the electrostatic interactions among charged ionizing groups and BGE ions, which are responsible of the IPCR phenomenon described previously in the literature [7-12]. Thus the pH sensed by any electrically charged chain is not necessarily equal to the bulk pH of the BGE. Therefore from [9], one can express $G_\alpha = G_\alpha^* + RT\ln X_\alpha + e\,N_A Z_\alpha \zeta_\alpha/2$, where N_A is the Avogadro constant, $R = N_A k_B$ is the gas constant, k_B is the Boltzmann

constant, e is the elementary charge and G_α^* is the reference chemical potential that depends on T and pH_α^*, and hence on C_o when the PPCR phenomenon becomes relevant (see below). Also Z_α is the net charge number and ζ_α is the mean field zeta (electrokinetic) potential of species α. Therefore for a given dimerization degree $\Delta G^{eff} = \Delta G^* + eN_A(Z_D\zeta_D - 2Z_M\zeta_M)/2$ is the effective free energy change, where $\Delta G^* = G_D^* - 2G_M^*$ is the conformational free energy change yielding $K = \exp(-\Delta G^{eff}/RT)$. Here the electrostatic free energy change ΔG^{el} due to the dimerization equilibrium, defined $\Delta G^{el} = eN_A(Z_D\zeta_D - 2Z_M\zeta_M)/2$, is sensitive to pH_α^* due to IPCR phenomenon (Supporting Information) expressed,

$$pH_\alpha^* \approx pH + e^2Z_\alpha/\{\ln(10)k_BT4\pi\varepsilon a_{H\alpha}(1+\kappa a_{H\alpha})\} \quad (1)$$

where $a_{H\alpha}$ is the hydrodynamic radius of specie α and $\kappa = (2Ie^2N_A10^3/\varepsilon k_BT)^{1/2}$ is the Debye-Hückel parameter. Equation (1) applies for analyte infinite dilution only. For increasing values of C_o, this equation must be modified when a pair of charged particles comes near one another, giving an additional shift in the pH_α^* due to the PPCR phenomenon. Assuming that interactions of pair particles of equal size predominate [4], the pH_α^* may be expressed as follows,

$$pH_\alpha^* \approx pH + e^2Z_\alpha\{1+e^{-\kappa d}\}/\{\ln(10)k_BT4\pi\varepsilon a_{H\alpha}(1+\kappa a_{H\alpha})\} \quad (2)$$

In this expression the average distance d between two particle centers of species α depends on C_o and the dimerization degree ξ, giving monomer $C_M = C_o - 2\xi$, dimer $C_D = \xi$ and total concentrations $C = C_o - \xi$. Therefore d may be estimated from $d \approx m(3/4\pi C N_A 10^3)^{1/3}$ involving peptide volume fraction in the solution at each ξ value. In this regard parameter m is obtained by assuming that charged particles are in a dynamic lattice having each cell a radius $r^* \approx (3/4\pi C N_A 10^3)^{1/3}$. Therefore $m \approx 1.207$ by considering that the average approach of pair interacting particles is between r^* and $\sqrt{2}\,r^*$ as derived from simple geometric calculations. In Eq. (2) the electrical potential of the interacting charged particles is $\psi_\alpha(d) \approx \zeta_\alpha\, e^{-\kappa d}$ as a first approximation, where the hypothesis of interacting effective point charges far from contact is introduced. For $C \to 0$ and $d \to \infty$, Eq. (1) is physically recovered at infinite dilution. Therefore, it is clear that the PPCR phenomenon introduces an additional shift of the pH_α^* toward the isoelectric point pI of species α chain, which is also a phenomenon controlling the interaction forces between peptides and proteins [3, 4, 25-27] as illustrated and discussed below in Section 3 for the peptide fragment under study. These approximations are used to illustrate simply the PPCR phenomenon and for clearness. A more precise numerical calculation may lead one to a difficult task, which is out of the purpose of the present work. From Eqs (1) and (2) one finds that the effective free energy must

depends on C_o, which is the formal demonstration that the aggregation of peptides is a concentration-dependent process (see also numerical validation below) because G_α depends on ζ_α as well as on pH_α^* including both the IPCR and PPCR phenomena. Therefore following our previous work [9] rewritten for this particular problem here, the molar fractions of monomer $X_M = (D - D_D)/(D_M - D_D)$ and dimer $X_D = (D_M - D)/(D_M - D_D)$ are obtained from the calculation of the mixture diffusion coefficient $D = X_D D_D + X_M D_M$. This last expression applies when the rate of interconversion from monomer to dimer of any chain in the solution is in the fast change regime, which indicates that the monomer and dimer mixture diffusion coefficient is an average value [9, 13, 43]. Then within the CE framework the effective electrophoretic mobility μ_α for $\alpha = M, D$ may be combined into an average mobility $\mu = \mu_M X_M + \mu_D X_D$, where μ is the effective electrophoretic mobility of monomer and dimer mixture of the AD plaque-competent Aβ(12-28) peptide fragment, while μ_M and μ_D are the effective electrophoretic mobilities of the monomer and dimer analogues, respectively, which are AD plaque-incompetent peptides fragment analogues, as expressed in [13].

2.2.2 Electrokinetic and hydrodynamic global properties

To evaluate the electrokinetic and hydrodynamic global properties of monomer and dimer analogues, the PLLCEM was used. Its applicability to polyampholyte-polypeptide chains has been discussed in detail in [3, 4, 7-12, 14, 15, 22, 25-27] by pointing out the approximations introduced. This model can be used with either diffusion coefficient or effective electrophoretic mobility values as input data (Supporting Information). Here diffusion coefficient experimental values $D_\alpha = k_B T/f_\alpha$ of species α reported in [13] are used to obtain friction coefficient f_α of monomer and dimer analogues (Supporting Information Table 1). Then the following electrokinetic and hydrodynamic global properties of monomer and dimer analogues with $\alpha = M$, D are obtained: effective $Z_\alpha = Z_{+\alpha} - |Z_{-\alpha}|$, positive $Z_{+\alpha}$, negative $Z_{-\alpha}$ and total $Z_{T\alpha}$ charge numbers, effective charge number fraction $\Delta\sigma_\alpha = |Z_\alpha|/N_\alpha$, total charge number fraction $\sigma_\alpha = Z_{T\alpha}/N_\alpha$, approximate hydration H_α (number of water molecules per chain) or δ_α (gram of water/gram of peptide), size estimated via the equivalent hydrodynamic or Stokes radius $a_{H\alpha}$, compact radius $a_{c\alpha}$ accounting the chain mass only, friction ratio Ω_α (also designated asphericity) where both the stick and slip between fluid and hydrated particle may be considered [27], pH near molecule designated pH^*_α due to both IPCR and PPCR phenomena. Therefore the estimation of μ_M, μ_D and μ are readily calculated as

indicated in the Supported Information and Section 2.1. In addition species α hydration is defined $H_\alpha = H_{o\alpha} + H_{d\alpha}$ [4], where $H_{o\alpha}$ is the number of water molecules captured by amino acid residues of the AAS, while $H_{d\alpha}$ is the number of water molecules due to the degree of water occlusion or release by peptides [4]. Concerning the physical interplay between particle shape and hydration described previously [4] one may consider the minimum δ_α sampled by the chain ($H_{d\alpha} = 0$ and $\Omega_\alpha < 1$) and the maximum δ_α physically admissible ($H_{d\alpha} > 0$ and $\Omega_\alpha = 1$). Further partial BGE slip on particle surface applies when $\Omega_\alpha > 1$ with $H_{d\alpha} = 0$ for both spherical and aspherical hydrated particles [4, 27]. In this case $H_{d\alpha} < 0$ is required to obtain BGE stick on particle surface with $\Omega_\alpha = 1$ as long as $a_{H\alpha} \geq a_{c\alpha}$ is satisfied.

3 Results and discussion

3.1 Electrokinetic and hydrodynamic global properties of monomer and dimer analogues

Supporting Information Table 2 shows main global properties of monomer and dimer analogues at pH 2.9 obtained within the framework of Section 2.2 for $H_{d\alpha} = 0$, when the IPCR phenomenon is included only (Eq. (1)). Although an extended set of properties are presented in this table, we will not describe fully this numerical information here because one may use [3, 4, 7-12, 14, 15, 22, 25-27] for direct interpretations. Instead this discussion section will be centered on

physical aspects considered relevant for the visualization of the mechanisms associated with the amyloidogenic process of interest in AD. Thus when the IPCR phenomenon is considered, the charge numbers of residual $Z_{AspM} \approx -0.49$, $Z_{GluM} \approx -0.28$, $Z_{ArgM} \approx 1.00$, $Z_{HisM} \approx 0.99$, $Z_{LysM} \approx 1.00$, and terminal $Z_{NH_2M} \approx 1.00$, $Z_{COOHM} \approx -0.60$ ionizing groups in the monomer analogue show that ionizing amino groups are fully protonated, while ionizing carboxylic groups are partially protonated yielding relatively a high effective charge number fraction $\Delta\sigma_M \approx 0.21$ [14, 15, 22]. In this regard, one expects an enough electrostatic repulsion among monomer analogue chains avoiding for instance the aggregation via salt bridges stabilized with beta-sheet conformations (this physical interchain interaction requires a very close approximation between particles of around 4 Å [44]). These quantitative results are consistent with the discussion in [13] and citations therein. In fact the dimerization of the monomer occurs mainly via hydrophobic forces associated with the central region LVFFA (the monomer analogue did not present dimerization at any C_o because this zone was changed to LVGGA). From this table one finds that $pH_M^* \approx 3.98$ is lower than $pH_D^* \approx 4.31$ while both monomer and dimer analogues present the same p*I* 7.09. It should be observed that at p*I*, charge regulation phenomena cancel out in polyampholyte chains [3, 4, 25, 26]. Therefore it is clear that the dimerization yielded a pH_D^* closer to the p*I* as a consequence of the IPCR

phenomenon (below in Section 3.3, it is shown that this shift is enhanced even more due to the PPCR phenomenon). The dimer analogue has $Z_{AspD} \approx -0.67$, $Z_{GluD} \approx -0.45$, $Z_{ArgD} \approx 1.00$, $Z_{HisD} \approx 0.99$, $Z_{LysD} \approx 1.00$, $Z_{NH_2D} \approx 1.00$ and $Z_{COOHD} \approx -0.76$, showing that ionizing amino groups remained fully protonated but ionizing carboxylic groups increased their negative charge numbers yielding relatively lower $\Delta\sigma_D \approx 0.18$, what imply less electrostatic intraparticle repulsion. Therefore the dimer seems to be a more stable particle than the monomer from the electrostatic point of view. This phenomenon may occur in the interactions of proteins and peptides in general. Its deeper elucidation and additional applications will be worth to be considered in future researches. In a forthcoming work we will show that this phenomenon is enhanced even more when oligomers of higher order are formed. This last aspect is also consistent with the fact that for pH>4 (nearer the p*I*) other higher oligomers must be consider for the Aβ(12-28) peptide fragment ending up in complex structures like protofibrils and fibrils typically found in AD [13, 45]. This result is not surprising taking into account that at higher protocol pH the monomer will approach closer the p*I* 7.09 due to the pH_M^* shift expected. On the other hand it is not simple to visualize how the monomer may have a good propensity to aggregation once the central hydrophobic nucleation occurs, unless it is a consequence of an additional pH near molecule shift toward the p*I* as explained and discussed above.

From Supporting Information Table 2, one also finds that $\Omega_\alpha > 1$ with $H_{d\alpha} = 0$ and the monomer and dimer analogues can be considered as sampling a spherical particle with partial BGE slip at the surface [27]. This result is probably associated with a poor packing of D_2O on the particle surface. The D_2O molar mass is higher than that of H_2O causing the "cage effect" already described previously in [27]. Further, when H_2O was considered as BGE in calculations, both Ω_α became near unity from below. Thus BGE stick condition was found showing that the apparent slip is due to solvent type used in the BGE formulation. This conclusion is reinforced with the fact that the monomer and dimer analogues are relatively low hydrophilic chains as indicated in the Supporting Information, and hence one does not expect a high slip as it was found mainly with hydrophobic chains in [27]. The discussion of this section may be readily extended to the cases when the monomer and dimer analogues are considered particles sampling the minimum hydration with $H_\alpha < 0$ as required to reduce $\Omega_\alpha > 1$ to $\Omega_\alpha = 1$ (Supporting Information Table 3).

3.2 Monomer and dimer mixture effective electrophoretic mobility and properties

Supporting Information Table 2 shows $\mu_M < \mu_D$ despite they are expect to be rather equal. There is a subtle phenomenon to be explained with this result by taking into account that from the experimental information in Ref. [13] $D_M > D_D$, which is the opposite relationship to that concerning effective

electrophoretic mobilities. Thus while $D_\alpha \propto 1/f_\alpha$ and the later inequality applies, one observes that $\mu_\alpha \propto Z_\alpha/f_\alpha$ (here hydration and IPCR phenomenon must be included [4]) permitting a different inequality. Therefore results in this table show that the dimerization of the monomer analogue yields a higher increase of effective charge number than an increase in friction coefficient. The explanation is that $pH_M^* < pH_D^*$ (3.98 compared to 4.31), as indicated above in Section 3.1, giving $Z_D \approx 6.19$ less than twice $Z_M \approx 3.62$. In addition, $\delta_M > \delta_D$ (0.55 compared to 0.51) affecting the volume size of the dimer and resulting in $f_D \approx 2.31 \times 10^{-11}$ kg/s less than twice $f_M \approx 1.66 \times 10^{-11}$ kg/s value. Consequently it is clear that in general global properties of the dimer cannot be taken twice those of the monomer due to both IPCR phenomenon and particle hydrations.

It must be also pointed out here that in general for high Z_α the ratio $e\zeta_\alpha/k_BT > 2.5$, which is a value around the onset of ion polarization-relaxation effects (see details in [14, 46, 47]) and μ_α may become saturated taking an asymptotic value at very high ζ_α. Nevertheless, the cases considered here presented $\kappa a_{H\alpha} < 0.02$ extending even more the admissible values of electrokinetic potentials [14].

Figure 1 shows the monomer and dimer mixture effective electrophoretic mobility μ as a function of C_o in relation to the monomer and dimer analogues μ_M and μ_D when the PPCR phenomenon has been neglected. For increasing C_o

it is clear that $\mu \to \mu_D$ (at $C_o \approx 3.25$ mM this peptide fragment is near the limit of solubility [13]) while the opposite is true for $C_o \to 0$ giving $\mu \to \mu_M$ (for $C_o < 0.5$ mM diffusion coefficient measurements presented low accuracy [13]). Thus the modified monomer and dimer in Ref. [13] are quite good analogues of the monomer and dimer associated with the Aβ(12-28) peptide fragment. Further, in relation to thermodynamic calculations, Supporting Information Table 4 shows how the dimerization degree, equilibrium constant and effective free energy change vary with C_o validating the theoretical reasoning and analysis given above in Section 2.1. This table also shows that ΔG^{eff} changes from positive to negative values (441.3 to -254.6 J/mol) at around $C_o \approx 1.25$-1.5 mM yielding a favorable free energy change to dimerization of the Aβ(12-28) peptide fragment when pH 2.9. Since $\Delta G^{eff} \approx 0$ for $C_o \approx 1.37$ mM, this initial monomer concentration value is a good estimate to indicate a significant nucleation for conversion to dimer of the peptide fragment giving $X_D \approx 0.383$. Further Supporting Information Figure 1 is equivalent to Figure 1 where μ, μ_M and μ_D are presented as a function of X_D where two extrapolating point are included at $X_D = 0$ and 1 to show the consistency of calculations in terms of dimer molar fractions [9, 43].

3.3 Effects of the PPCR phenomenon for increasing initial monomer concentration

Figure 2 shows the mixture effective electrophoretic mobility μ as a function of C_o in relation to the monomer and dimer analogues μ_M and μ_D when both IPCR and PPCR phenomena are considered in calculations (Eq. (2)). Once more for low and high C_o the expected asymptotic tendencies of μ are observed. Nevertheless the monomer and dimer analogues effective electrophoretic mobilities decrease with higher values of C_o as a consequence of the inclusion of the PPCR phenomenon coupled also to particles hydration. The differences found in the comparison between Figure 1 and 2 demonstrate the relevance of the PPCR phenomenon when two peptides approach one another at higher C_o values. To complement the illustration of the rapid interconversion rates of chains in the dimerization process, the change of the mixture effective charge number $Z = Z_M X_M + Z_D X_D$ with C_o is shown in the Supporting Information Figure 2.

At each increment of C_o, the PPCR phenomenon introduces an additional near molecule pH shifts in the calculation of the pH_α^* previously shown in the Supporting Information Table 2. This effect is illustrated in Figure 3 where pH_α^* as a function of C_o due to PPCR phenomenon is shown. In fact, at infinite dilution $pH_M^* \to 3.98$ consistently with the theory of Section 3.1, while at the

higher C_o, the monomer analogue particles become closer and the pH_M^* increases by reaching a value around 4.31, which is the pH_D^* value when the PPCR phenomenon is neglected while the IPCR phenomenon is considered. In this regard the pH_D^* shift of the dimer analogue due to the PPCR phenomenon changes from 4.31 at infinity dilution to 4.66 at around $C_o \approx 3.25$ mM as shown in Figure 3, which cannot convert to higher oligomers at pH<4 as indicated above. Further for $d \to 0$ the contact of two monomers may produce a dimer and the merged particles are not anymore kinematically independent. Figure 3 also illustrates the estimations of distances between pair of monomer analogue particles when C_o increases. For $C_o \approx 3.25$ mM a distance of around three particle diameters are obtained. In this regard, these calculations are simpler for the dimer (merged particles) than for the two monomers in near contact at high C_o where Eq. (2) may start to be invalid [4]. Full sets of numerical calculations related to the inclusion of the PPCR phenomenon are available in Supporting Information Tables 5 and 6 for a better analysis of Figures 2 and 3. Results illustrate that the dimerization of the Aβ(12-28) peptide fragment is induced when a substantial average approach among the hydrated particles is achieved by increasing C_o. In this regard the PPCR phenomenon is relevant in this process, in opposition to what happens at infinity dilution, by introducing a pH_α^* shift toward the pI additional to that caused by the IPCR phenomenon. From

these approximate calculations it is also clear that the PPCR phenomenon deserves special consideration in the interaction between proteins and peptides in general. Therefore further research is needed to completely elucidate this subtle phenomenon.

Finally it is important to point out that the nucleation of the dimerization process via the central hydrophobic region LVFFA is facilitated by the pH_{α}^{*} shifts toward the pI as C_o increases, which partially reduce the interparticle electrostatic repulsion. Also one has to observe that the wild effective charge number $Z_{w\alpha}$ is higher than the regulated effective charge number Z as depicted in Supporting Information Tables 2, 3, 5 and 6 [3, 4, 25, 26].

4 Concluding Remarks

The effective electrophoretic mobility is one of the relevant transport properties of amyloid-beta peptides to be measured at appropriate BGE compositions with the purposed of studying the amyloidogenic process. The pH_{α}^{*} shifts toward the peptide pI is a consequence of both the IPCR and PPCR phenomena enhancing the oligomerization of the Aβ(12-28) peptide fragment via the hydrophobic region LVFFA studied here at pH 2.9. These phenomena may be important mechanisms causing the amyloidogenic process of amyloid beta peptides leading to the neuronal plaque formations at higher pH values by reducing repulsion electrostatic forces between chains. To deepen this aspect, additional researches involving CE experimental studies of these peptides are

required. Our forthcoming manuscript will show that higher order oligomerization of amyloid-beta peptides is consistent with the results found here involving the IPCR and PPCR phenomena.

Acknowledgements

Authors wish to thank the financial aid received from Universidad Nacional del Litoral, Santa Fe, Argentina (CAI+D-2011) and CONICET (PIP-112-201101-00060).

The Authors have declared no conflict of interest.

5 References

[1] Hearn, M. T. W., Keah, H. H., Boysen, R. I., Messana, I., Misiti, F., Rossetti, D. V., Giardina, B., Castagnola, M., *Anal. Chem.* 2000, *72*, 1964-1972.

[2] Chiti, F., Dobson, C. M., *Annu. Rev. Biochem.* 2006, *75*, 333-366.

[3] Deiber, J. A., Piaggio, M. V., Peirotti, M. B., *Electrophoresis* 2014, *35*, 755-761.

[4] Deiber, J. A., Piaggio, M. V., Peirotti, M. B., *J. Sep. Sci.* 2014, *37*, 2618-2624.

[5] Blennow, K., Hampel, H., Weiner, M., Zetterberg, H., *Nat. Rev. Neurol*. 2010, *6*, 131-144.

[6] Masters, C. L., Selkoe, D. J., *Cold Spring Harb. Perspect. Med*. 2012, 2: a006262.

[7] Piaggio, M. V., Peirotti, M. B., Deiber, J. A., *Electrophoresis* 2005, *26*, 3232-3246.

[8] Piaggio, M. V., Peirotti, M. B., Deiber, J. A., *Electrophoresis* 2006, *27*, 4631-4647.

[9] Piaggio, M. V., Peirotti, M. B., Deiber, J. A., *Electrophoresis* 2007, *28*, 2223-2234.

[10] Piaggio, M. V., Peirotti, M. B., Deiber, J. A., *Electrophoresis* 2007, *28*, 3658-3673.

[11] Peirotti, M. B., Piaggio, M. V., Deiber, J. A., *J. Sep. Sci.* 2008, *31*, 548-554.

[12] Piaggio, M. V., Peirotti, M. B., Deiber, J. A., *Electrophoresis* 2009, *30*, 2328-2336.

[13] Mansfield, S. L., Jayawickrama, D. A., Timmons, J. S., Larive, C. K., *Biochim. Biophys. Acta* 1998, *1382*, 257-265.

[14] Piaggio, M. V., Peirotti, M. B., Deiber, J. A., *J. Sep. Sci.* 2010, *33*, 2423-2429.

[15] Deiber, J. A., Piaggio, M. V., Peirotti, M. B., *Electrophoresis* 2012, *33*, 990-999.

[16] Šolínová, V., Kašička, V., Koval, D., Hlaváček, J., *Electrophoresis* 2004, *25*, 2299-2308.

[17] Simó, C., González, R., Barbas, C., Cifuentes, A., *Anal. Chem*. 2005, *77*, 7709-7716.

[18] Benavente, F., Balaguer, E., Barbosa, J., Sanz-Nebot, V., *J. Chromatogr. A* 2006, *1117*, 94-102.

[19] Šolínová, V., Kašička, V., Sázelová, P., Barth, T., Mikšík, I., *J. Chromatogr. A* 2007, *1155*, 146-153.

[20] Allison, S. A., Pei, H., Allen, M., Brown, J., Chang-II, K., Zhen, Y., *J. Sep. Sci.* 2010, *33*, 2439-2446.

[21] Aptisa, G., Benavente, F., Sanz-Nebot, V., Chirila, E., Barbosa, J., *Anal. Bioanal. Chem*. 2010, *396*, 1571-1579.

[22] Deiber, J. A., Piaggio, M. V., Peirotti, M. B., *Electrophoresis* 2011, *32*, 2779-2787.

[23] Allison, S. A., Perrin, C., Cottet, H., *Electrophoresis* 2011, *32*, 2788-2796.

[24] Wu, H. F., Allison, S. A., Perrin, C., Cottet, H., *J. Sep. Sci.* 2012, *35*, 556-562.

[25] Deiber, J. A., Piaggio, M. V., Peirotti, M. B., *Electrophoresis* 2013, *34*, 700-707.

[26] Deiber, J. A., Piaggio, M. V., Peirotti, M. B., *Electrophoresis* 2013, *34*, 708-715.

[27] Deiber, J. A., Piaggio, M. V., Peirotti, M. B., *Electrophoresis* 2013, *34*, 2648-2654.

[28] Šolínová, V., Kašička, V., *Electrophoresis* 2013, *34*, 2655-2665.

[29] Allison, S. A., Wu, H., Bui, T. M., Dang, L., Huynh, G. H., Nguyen, T., Soegiarto, L., Truong, B. C., *J. Sep. Sci.* 2014, *37*, 2403-2410.

[30] Kašička, V., *Electrophoresis* 2012, *33*, 48-73.

[31] Selvaraju, S., El Rassi, Z., *Electrophoresis* 2012, *33*, 74-88.

[32] Righetti, P. G., Sebastiano, R., Citterio, A., *Proteomics* 2013, *13*, 325-340.

[33] Kašička, V., *Electrophoresis* 2014, *35*, 69-95.

[34] Ali, I., Al-Othman, Z. A., Al-Warthan, A., Asnin, L., Chudinov, A., *J. Sep. Sci*. 2014, *37*, 2447-2466.

[35] Verpillot, R., Otto, M., Klafki, H., Taverna, M., *J. Chromatogr. A* 2008, *1214*, 157-164.

[36] Sabella, S., Quaglia, M., Lanni, C., Racchi, M., Govoni, S., Caccialanza, G., Calligaro, A., Bellotti, V., De Lorenzi, E., *Electrophoresis* 2004, *25*, 3186-3194.

[37] Kato, M., Kinoshita, H., Enokita, M., Hori, Y., Hashimoto, T., Iwatsubo, T., Toyo'oka, T., *Anal. Chem*. 2007, *79*, 4887-4891.

[38] Colombo, R., Carotti, A., Catto, M., Racchi, M., Lanni, C., Verga, L., Caccialanza, G., De Lorenzi, E., *Electrophoresis* 2009, *30*, 1418-1429.

[39] Picou, R. A., Moses, J. P., Wellman, A. D., Kheterpal, I., Gilman, S. D., *Analyst (Cambridge, United Kingdom)* 2010, 135, 1631-1635.

[40] Picou, R. A., Kheterpal, I., Wellman, A. D., Minnamreddy, M., Ku, G., Gilman, S. D., *J. Chromatogr. B* 2011, *879*, 627-632.

[41] Verpillot, R., Esselmann, H., Mohamadi, M. R., Klafki, H., Poirier, F., Lehnert, S., Otto, M., Wiltfang, J., Viovy, J. L., Taverna, M., *Anal. Chem.* 2011, *83*, 1696-1703.

[42] Pryor, N. E., Moss, M. A., Hestekin, Ch. N., *Int. J. Mol. Sci.* 2012, *13*, 3038-3072.

[43] Verzola, B., Fogolari, F., Righetti, P. G., *Electrophoresis* 2001, *22*, 3728-3735.

[44] Kumar, S., Nussinov, R., *ChemBioChem* 2002, *3*, 604-617.

[45] Fraser, P. E., Nguyen, J. T., Surewicz, W. K., Kirschner, D. A., *Biophys. J.* 1991, *60*, 1190-1201.

[46] Allison, S. A., *Macromolecules* 1996, *29*, 7391-7401.

[47] Allison, S. A., *Biophys. Chem.* 2001, *93*, 197-213.

Figure 1. Monomer μ_M (■) and dimer μ_D (□) analogues and monomer and dimer mixture μ (∗) effective electrophoretic mobilities as a function of initial monomer concentration C_o. Results are from the PLLCEM at pH 2.9, I = 1 mM and 25ºC when the hydrated particle sampled is spherical with BGE slip. The IPCR phenomenon is considered only.

Figure 1

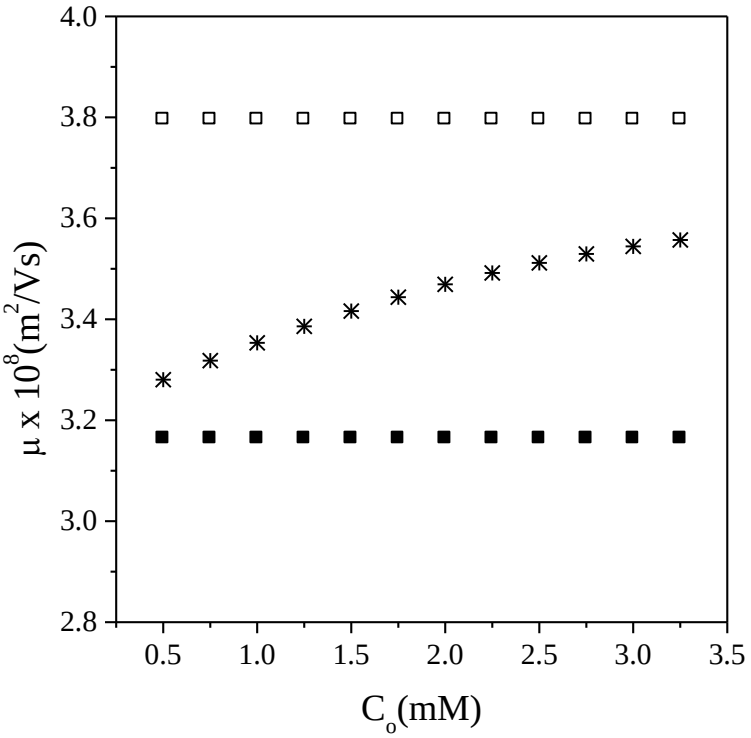

Figure 2. Monomer μ_M (■) and dimer μ_D (□) analogues and monomer and dimer mixture μ (∗) effective electrophoretic mobilities as a function of initial monomer concentration C_o. Results are from the PLLCEM at pH 2.9, I = 1 mM and 25ºC when the hydrated particle sampled is spherical with BGE slip. The IPCR and PPCR phenomena are considered.

Figure 2

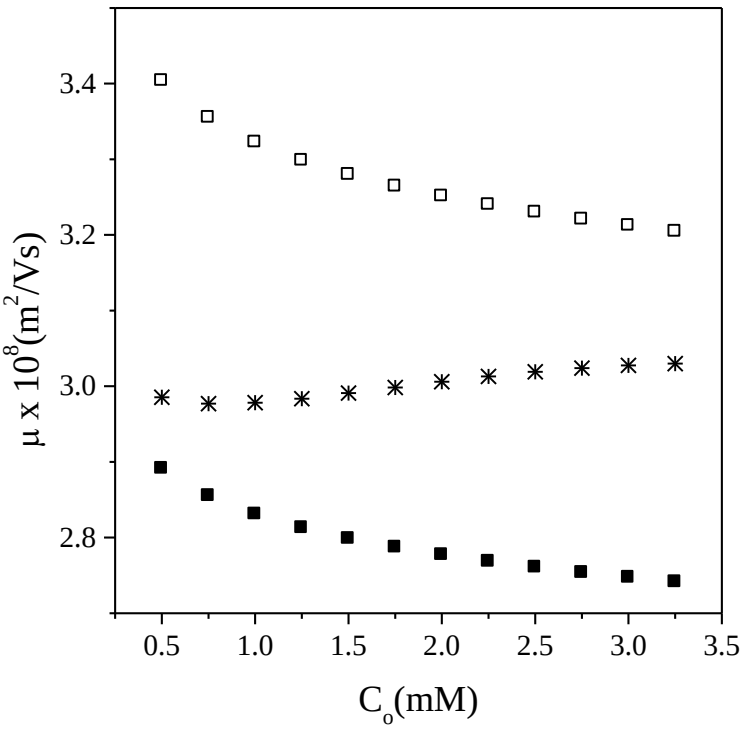

Figure 3. pH_{α}^{*} shifts toward pI of monomer (■) and dimer (□) analogues and distance between particles d (○) as a function of initial monomer concentration C_o when the IPCR and PPCR phenomena are considered. Results are from the PLLCEM at pH 2.9, I = 1 mM and 25ºC when the hydrated particle sampled is spherical with BGE slip.

Figure 3